Influence of aluminum substitution on the vortex matter properties of MgB_2

M. Pissas,[1] D. Stamopoulos,[1] N. Zhigadlo,[2] and J. Karpinski[2]
[1]*Institute of Materials Science, NCSR, Demokritos, 15310 Aghia Paraskevi, Athens, Greece*
[2]*Laboratory for Solid State Physics, ETH, 8093 Zürich, Switzerland*
(Received 28 June 2006; revised manuscript received 21 March 2007; published 29 May 2007)

The vortex matter phase diagrams of aluminum doped $Mg_{1-x}Al_xB_2$ crystals, deduced from local Hall ac-susceptibility (for $\mathbf{H}\|c$ axis) and bulk dc-magnetization measurements (for $\mathbf{H}\|c$ axis and *ab* plane) are reported. As in pristine and carbon doped MgB_2, aluminum substituted crystals display the peak effect in the critical current. The peak effect is located very close to the $H_{c2}^c(T)$ line, while it disappears below a characteristic magnetic field H^* that depends on Al content. The absence of significant bulk pinning below the onset of the peak effect implies that the Bragg glass phase is present there. In some of the crystals the peak effect is not present as a sharp negative peak of the real part of the local ac susceptibility, but it appears as a negative double-peak feature. This observation may be related with the miscibility gap that occurs for $0.05 \leqslant x \leqslant 0.5$. For low aluminum content the $H_{c2}^c(T)$ line lies slightly above the corresponding one of the pristine MgB_2, but for higher aluminum content, T_c, $H_{c2}^{ab,c}(0)$, and anisotropy parameter $\gamma = H_{c2}^{ab}(0)/H_{c2}^c(0)$ take lower values when compared to pristine MgB_2. Similarly with the pristine MgB_2 crystals for the superconducting aluminum substituted crystals, the anisotropy parameter decreases monotonously as temperature increases as well. All the experimental observations could be qualitatively explained within the clean two-band approximation.

DOI: 10.1103/PhysRevB.75.184533 PACS number(s): 74.25.Dw, 74.25.Ha, 74.25.Op, 74.62.Bf

I. INTRODUCTION

Since the discovery of superconductivity in MgB_2 compound[1] a vast amount of experimental and theoretical effort has been devoted to the comprehensive understanding of the physical mechanism being responsible for the superconductivity in MgB_2. Band-structure calculations[2] have shown that four bands cross the Fermi level of the MgB_2. Two of these bands are formed by in-plane σ sp^2 hybridized orbitals stretched along boron-boron bonds and are two dimensional (2D), hole type, and strongly coupled with the optical E_{2g} phonon mode. The other two are more isotropic, three-dimensional (3D) honeycomb shaped sheets, formed from out-of-plane π bonding and antibonding p_z orbitals of boron. These bands are weakly coupled to the phonons. The charge carriers in one of them are electronlike and in the other one holelike. This complicated Fermi surface topography leads into two distinct *s*-wave superconducting gaps.[3] The most evident consequence of the two-gap superconductivity of pristine MgB_2 is the temperature dependencies of the anisotropy parameters $\gamma_\xi = \xi_{ab}/\xi_c$ and $\gamma_\lambda = \lambda_c/\lambda_{ab}$. This behavior differs from that of one-gap superconductors where these two anisotropic parameters are usually equal and temperature independent.[4]

Methodologically, the elucidation of the superconductivity mechanism, as well as the vortex matter properties, usually include atomic substitution studies. Atomic substitutions may influence the properties of a superconductor relevant with the critical current, thus making it appropriate for practical applications, by increasing the $H_{c2}(T)$ line and/or the critical current that the superconductor can sustain without exhibiting losses. Additionally, they may also help in the clarification of the superconductivity mechanism. In MgB_2 atomic substitutions change the impurity scattering rates, the electron-phonon interaction, and the electron density. The existence of σ and π bands results in three different impurity scattering channels, namely intraband (σ and π) and interband scattering. One of the fundamental differences expected between a multiband superconductor and a conventional *s*-wave one-band superconductor, as far as the substitution effects are concerned, is that nonmagnetic impurities may act as Cooper pair breakers, due to the interband scattering which mixes the Cooper pairs in the two different bands.[5–7] Consequently, in a two-band superconductor the atomic substitutions could lead to reduction of T_c both by increasing the interband scattering and/or from the effect of electron doping on the electronic structure (modification of the density of states and electron-phonon interaction).

Until now, carbon[8–19] and aluminum[20–29] substitutions have been studied in appreciable detail. Since carbon substitutes boron, it is expected that it induces large interband scattering.[7] On the other hand, aluminum atoms substitute Mg, producing out-of-plane distortions of the boron atoms in neighboring planes which in turn mix the in-plane $p_{x,y}$ and out-of-plane p_z orbitals, which can increase the σ-π scattering.[6] Both substitutions produce a similar decrease in T_c, but the influence on the H_{c2} is different. Carbon substitution increases H_{c2} substantially while Al mainly causes the opposite. Single-crystal and powder sample studies have shown that the substitution of Mg for Al in MgB_2 produces single phase materials only for $x < 0.15$ and $0.5 < x < 1$. In the intermediate concentration regime ($0.15 < x < 0.5$) the samples show a tendency for phase separation. For $x \sim 0.5$ a superstructure is thermodynamically more stable with unit cell doubled along the *c* axis which arises from the ordering of the Mg and Al.[30] The gradual decreasing of T_c upon substitution of Mg for Al and of B for C, has been attributed mainly to the density of states decreasing at the Fermi level induced by electron doping and reduced lattice volume rather than increasing interband scattering. Recently, high quality aluminum substituted crystals has been grown using a high-pressure technique.[31] Bulk resistivity and magnetic measure-

ments showed that the upper critical filed for $\mathbf{H}\|c$ for small aluminum concentration slightly increases while for higher concentrations both H_{c2}^{ab}, H_{c2}^{c}, and anisotropy parameter γ_ξ are reduced in comparison with the pristine MgB_2. In addition, point-contact measurements of the energy gaps in $Mg_{1-x}Al_xB_2$ single crystals with $0.02 \leqslant x \leqslant 0.21$ showed no merging of the gaps down to 20 K.[31]

The aim of the present paper is to study the influence of aluminum substitution on the vortex matter properties of MgB_2 single crystals. The important new findings of our study are the following: (i) the anisotropy of H_{c2} decreases for low aluminum content; (ii) while for low aluminum content $H_{c2}^{c}(T)$ increases, for a higher amount it decreases, in comparison to pristine MgB_2; (iii) similarly to pristine MgB_2, we observed the peak effect in the critical current for all the studied single crystals; (iv) in some of the studied crystals we observed a double-peak structure in the critical current which may be an indication for inhomogeneous aluminum distribution (phase separation).

II. EXPERIMENTAL DETAILS

Al substituted MgB_2 crystals were grown in Zürich using a high-temperature pressure method.[31] The amount of aluminum content was determined by energy dispersive x-ray in the 4-5 place of the crystal surface. The average aluminum content (x) was found lower than in the precursor and depends on the precursor composition and the growth temperature.[31] Local ac susceptibility and global magnetization were carried out on three $Mg_{1-x}Al_xB_2$ single crystals with average aluminum content $x=0.013\pm0.006$ ($V\approx600\times400\times15$ μm^3), 0.101 ± 0.01 ($V\approx900\times500\times15$ μm^3), and 0.141 ± 0.004 ($V\approx780\times440\times15$ μm^3) for batches AN369, AN363, and AN392, respectively.

The local ac susceptibility was measured using a GaAsIn Hall sensor (active area of 50×50 μm^2) with dc and ac magnetic fields parallel to the c axis of the crystal ($\mathbf{H}_{dc}\|\mathbf{H}_{ac}\|c$ axis). In order to measure the small ac field in the presence of a large dc magnetic field, a second sensor of the same size was connected in opposition to the first one by means of an ac bridge. This effectively nulls the contribution of the dc field. The real and imaginary parts ($V=V'+iV''$) of the modulated Hall voltage ($f=3$ Hz), which are proportional to the local magnetic moment ($V_{ac}\propto m_{ac}\propto B_{ac}-H_{ac}$) at the surface of the crystal, were measured using two lock-in amplifiers. The low-temperature high-field measurements were carried out in a 100-kOe OXFORD cryostat. Global dc-magnetization measurements were carried out using a superconducting quantum interference device (SQUID) magnetometer (Quantum Design).

III. EXPERIMENTAL RESULTS

In Fig. 1 we show the temperature variation of the real (χ') and imaginary (χ'') parts of the local ac susceptibility, measured in an ac field $H_{ac}=17$ Oe and several dc-magnetic fields for the crystal with $x=0.013$. For low dc fields (see curves with $H_{dc}=10$, 15, and 17.5 kOe in Fig. 1) χ' reduces monotonically for $T<T_{c2}$, whereas the corresponding χ''

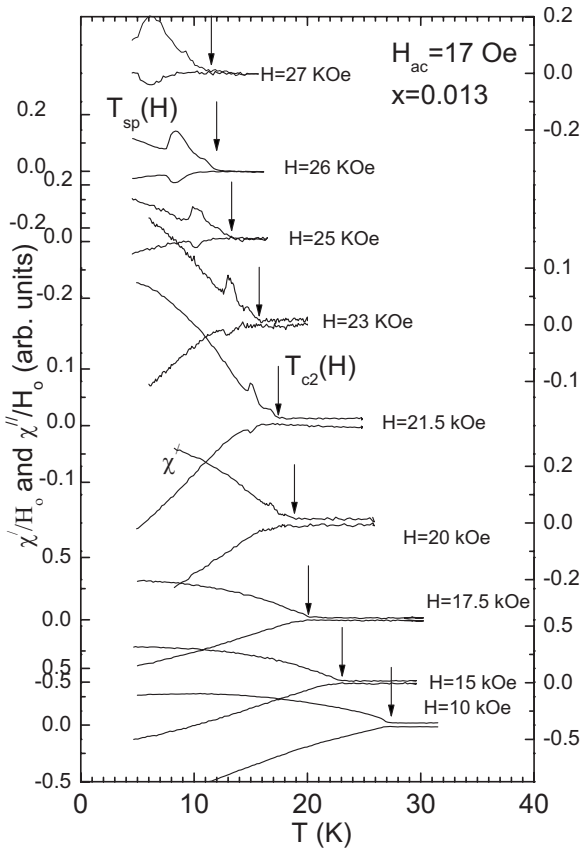

FIG. 1. Temperature variation of the real (χ') and imaginary (χ'') fundamental local ac susceptibility measured in the indicated magnetic dc fields of the $Mg_{1-x}Al_xB_2$ ($x=0.013$) single crystal, for $\mathbf{H}_{dc}\|\mathbf{H}_{ac}\|c$ axis. With arrows denoted are the $T_{c2}(H_{c2}^{c}=H_{dc})$.

forms a peak, whose location depends on the amplitude of the ac field and the temperature variation of the critical current density $J_c(H,T)$ [$H_{ac}\sim4\pi J_c(H,T_{peak})d$, here d is the thickness of the crystal]. From the measurements of Fig. 1 we can conclude that the $x=0.013$ crystal (as well as the others) have lower critical current, in comparison with the pristine and carbon substituted crystals.[15,32] The particular temperature variation of χ' and χ'' is typical for a type-II superconductor with a critical current increasing as temperature decreases (monotonous behavior). The diamagnetic onset in low-frequency ac-susceptibility measurements corresponds[33] to the low current density ($\mathbf{J}$) zero resistance, measured in a magnetic field ($\mathbf{H}\perp\mathbf{J}$). Therefore we attribute the onset temperature of the diamagnetic ac susceptibility χ' to the transition from normal to mixed superconducting state T_{c2} ($H_{dc}=H_{c2}^{c}$). The χ' for $H_{dc}=21.5$ kOe clearly displays a nonmonotonous temperature variation. Specifically, just below T_{c2} two negative peaks appear. Obviously, these peaks are related to the so-called peak effect in the critical current density J_c. The peak effect has also been observed in pristine MgB_2,[32,34] and carbon doped MgB_2.[15] The peak effect has also been observed in classical low-T_c superconductors like Nb,[35] V_3Si,[36] Nb_3Sn,[37] $NbSe_2$,[38,39] intermediate-T_c superconductor $(K,Ba)BiO_3$,[40] and all high-T_c superconductors, $Bi_2Sr_2CaCu_2O_{8+\delta}$,[41] $HgBa_2CuO_4$,[42] and $YBa_2Cu_3O_7$.[43–46] It is interesting to note that the dip of χ' at the peak-effect

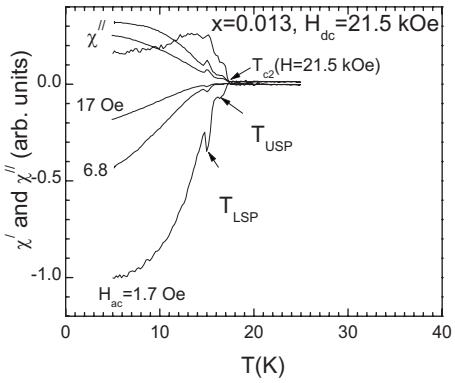

FIG. 2. Temperature variation of the local ac susceptibility measured in the indicated ac magnetic fields and $H_{dc}=21.5$ kOe of the $Mg_{1-x}Al_xB_2$ ($x=0.013$) single crystal for $\mathbf{H}_{dc}\|\mathbf{H}_{ac}\|c$ axis.

temperature is only a small fraction of the full, diamagnetic signal. This behavior is different from the one observed in carbon doped single crystals where at the region of the peak effect complete screening was observed.[15] Peak effect has also recently been reported in Ref. 33 for $H>15$ kOe, in a crystal with nominal composition $Mg_{0.88}Al_{0.12}B_2$.

Figure 2 shows the dependence of the local ac susceptibility on the applied ac field for the $x=0.013$ crystal. The arrows denote the onset temperature of the peak effect (T_{on}) and the temperature location of the lower and upper parts of the second peak (T_{LSP}, T_{USP}), respectively. The onset and the location of the dip are independent of H_{ac}. As the ac field becomes smaller the dip at the peak temperature becomes comparable with the diamagnetic screening χ' at $T=0$ K. This behavior is also observed in higher dc fields, as one can see in Fig. 1. The latter behavior implies that the critical current at the peak field (H_{SP}) increases as the temperature is lowered.

Figure 3 shows the temperature variation of χ' and χ'', measured in several dc magnetic fields of the $x=0.101$ crystal. As for the $x=0.013$, crystal, the ac-susceptibility data, in the field range $H>H^*\sim 10$ kOe, show a complicated behavior arising from several peaks in the critical current, right below the H_{c2}^c line. In this crystal (see measurements for $H=21$ kOe) one can clearly see two local minima [lower second peak (LSP) and upper second peak (USP)] on the $\chi'(T)$ curve, denoted as T_{LSP} and T_{USP}, and a very small feature between them. This complicated behavior is observed for $H>10$ kOe, whereas for lower dc fields it is transformed to a broad shoulder.

Figure 4 shows the local ac-susceptibility measurements of the crystal with $x=0.141$. This sample has lower $T_c=26.67$ K in comparison with the other crystals. Basically, this sample displays similar behavior with the other samples as far the ac susceptibility measurements are concerned. For $H>H^*\sim 15$ kOe the χ' right below the diamagnetic onset displays nonmonotonous behavior which can be accounted for by the peak effect as the pristine, $x=0.013$ and $x=0.101$ single crystals. Remarkably, the particular crystal shows only one dip in the χ' implying that only one peak value of the critical current occurs. Furthermore, comparing the value of χ' at the peak's maximum and the extrapolated at $T=0$, we

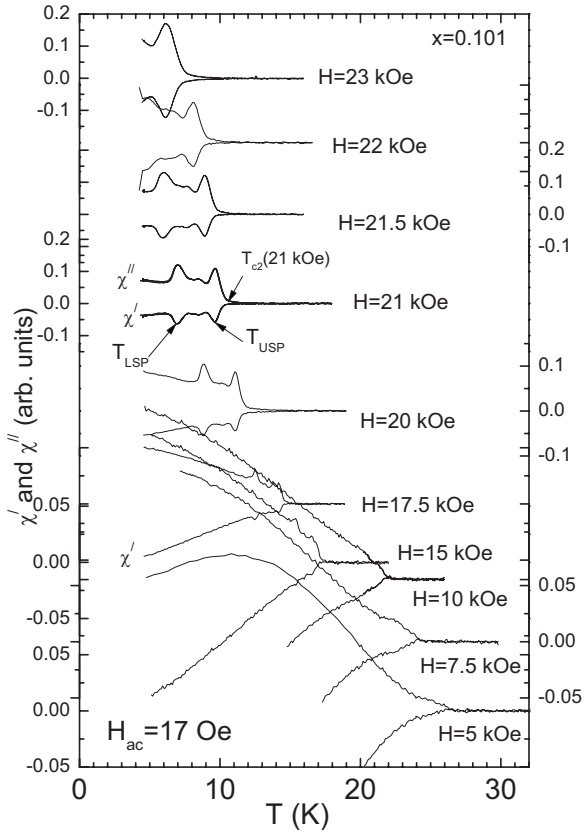

FIG. 3. Temperature variation of the real (χ') and imaginary (χ'') fundamental local ac susceptibility measured in the indicated magnetic dc fields of the $Mg_{1-x}Al_xB_2$ ($x=0.101$) single crystal, for $\mathbf{H}_{dc}\|\mathbf{H}_{ac}\|c$ axis.

conclude that the critical current of the particular crystal is significantly lower than the one of the crystals with $x=0$, 0.013, and 0.101.

Figure 5 summarizes the experimental results in the form of vortex-matter phase diagrams, for the $Mg_{1-x}Al_xB_2$ crystals with $x=0.0$, 0.013 [panel (a)], $x=0.101$ [panel (b)], and $x=0.141$ [panel (c)]. The open, solid, and semisolid circles in Figs. 5(a) and 5(b) correspond with the onset of the LSP (H_{on}), the LSP (H_{LSP}), the USP (H_{USP}), and the second peak (H_{SP}) lines for crystals $x=0.013$, 0.101, and 0.141, respectively. Similarly with pristine[32] and carbon substituted[15] MgB_2, all these lines for the crystals with $x=0.013$, 0.101, and 0.141 converge intersecting the $H_{c2}^c(T)$ line at (T^*, H^*) shown by a large solid circle in Figs. 5(a) and 5(c). For the crystal with $x=0.101$ it is difficult to define this point. In addition, Fig. 5 illustrates the temperature variation of the $H_{c2}^c(T)$ and $H_{c2}^{ab}(T)$ lines as measured by means of local ac susceptibility and bulk magnetization measurements. For comparison reasons we also included the $H_{c2}^c(T)$ line of the pristine MgB_2 crystal (grown by the same method) as it was estimated from SQUID measurements. Although the difference is small, the $H_{c2}^c(0)$ value for the $x=0.013$ sample is larger than the corresponding value for the $x=0.0$ sample. The upper critical field $H_{c2}^c(T)$ for $x=0.013$ and 0.101 crystals follows a nearly conventional temperature variation, while $H_{c2}^{ab}(T)$ displays a pronounced positive curvature near

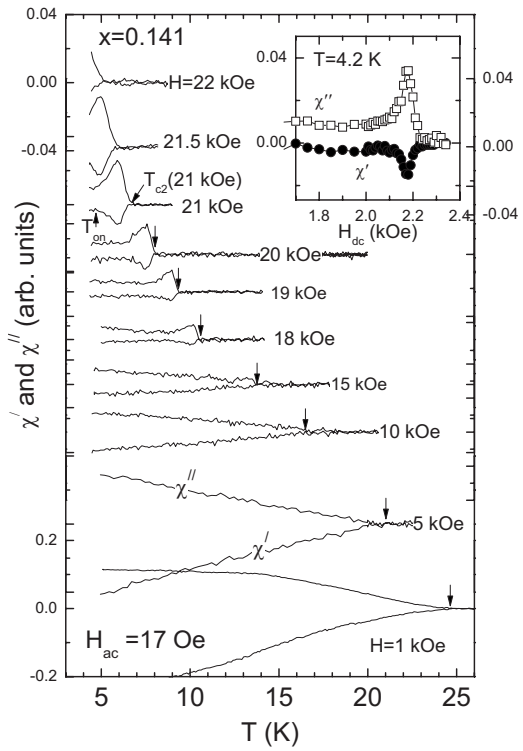

FIG. 4. Temperature variation of the real (χ') and imaginary (χ'') fundamental local ac susceptibility measured in the indicated magnetic dc fields of the $Mg_{1-x}Al_xB_2$ (x=0.141) single crystal, for $\mathbf{H}_{dc}\|\mathbf{H}_{ac}\|c$ axis. The inset shows $\chi\prime$ and χ'' as a function of the dc magnetic field, at T=4.2 K.

T_c. The positive curvature is related to the two-band superconductivity of MgB_2 and generally it is expected to be most pronounced in clean materials where electronic microscopic details affect the bulk properties such as the upper critical fields. In dirty materials impurity scattering smooths out these electronic details, producing linear temperature variation of the upper-critical fields. At this point we would like to note that the corresponding lines for the carbon substituted MgB_2 show a nearly linear behavior near T_c (see Ref. 15).

The experimental points for both $H^c_{c2}(T)$ and $H^{ab}_{c2}(T)$ can be least squares fitted by using the empirical formula $H_{c2}(T)=H_{c2}(0)[1-(T/T_c)^n]^\nu$ for all samples. The fitted parameters are summarized in Table I. In the context of Ginsburg-Landau theory, for anisotropic type-II superconductors, both $H^{ab,c}_{c2}$ are linear near T_c, e.g., $H_{c2}\propto(T_c-T)$. This particular temperature variation produces a temperature-independent anisotropy parameter, $\gamma=H^{ab}_{c2}/H^c_{c2}$. In the two-band superconductor the situation is radically different, where positive curvature terms [e.g., $H_{c2}\propto(T_c-T)^n$, $n\geqslant 2$] are present. These terms essentially produce the temperature variation of γ. In our case we decided to use the empirical relation $H_{c2}(T)=H_{c2}(0)[1-(T/T_c)^n]^\nu$, in order to reproduce the positive (negative) curvature observed near T_c (T=0), respectively.

Using the fitting equations for the $H^{ab}_{c2}(T)$ and $H^c_{c2}(T)$ we calculate the temperature variation of the anisotropy parameter $\gamma(T)$, which is depicted in the insets of Fig. 5. Here we must stress that the calculated γ originates from experimen-

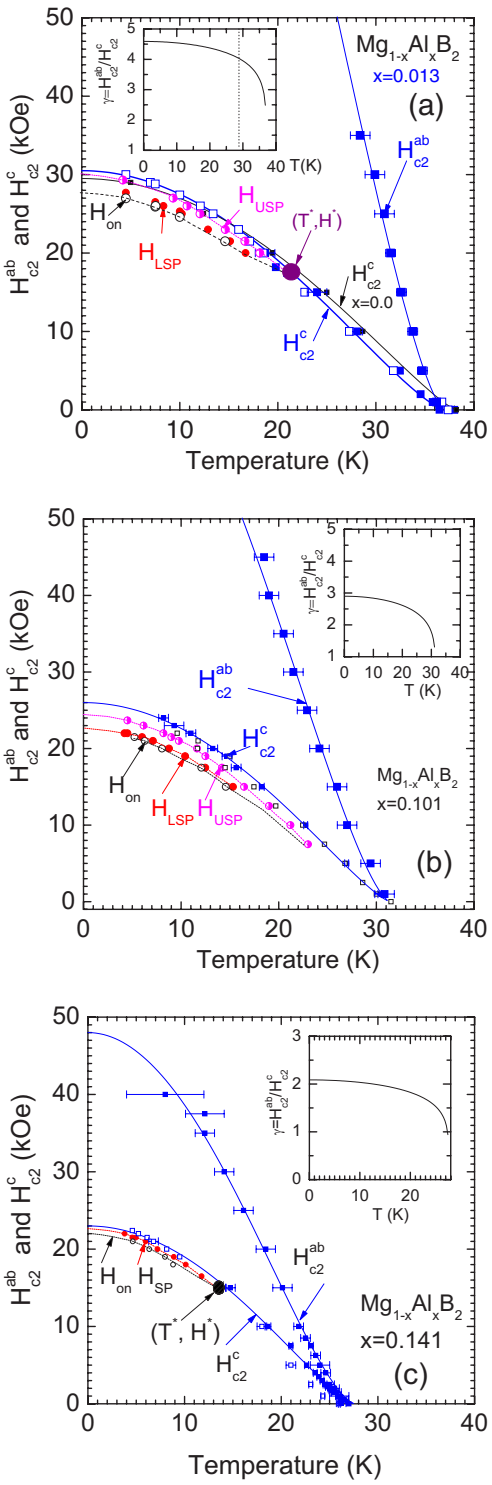

FIG. 5. (Color online) The vortex matter phase diagrams of single crystals $Mg_{1-x}Al_xB_2$ with x=0.0 (only H^c_{c2} is shown), 0.013 (a), x=0.101 (b), and x=0.141 (c). The open, solid, and semifilled circles correspond to the onset line (H_{on}), the low second peak line (H_{LSP}), the upper second peak line (H_{USP}), and the second peak line (H_{SP}) for crystals with x=0.013, 0.101, and 0.141, respectively. The dashed lines through the $H_{on}(T)$, $H_{LSP}(T)$, $H_{USP}(T)$, and $H_{SP}(T)$ data are to guide the eye. The solid (open) squares correspond to the critical fields $H^{ab,c}_{c2}(T)$, estimated from SQUID (Hall) measurements. The insets show the T variation of the $\gamma=H^{ab}_{c2}/H^c_{c2}$.

TABLE I. Least-square estimated parameters for both $H_{c2}^{c}(T)$ and $H_{c2}^{ab}(T)$ using the empirical formula $H_{c2}(T)=H_{c2}(0)[1-(T/T_c)^n]^{\nu}$. Numbers in parentheses are statistical errors referring to the last significant digit.

x	0.0	0.013	0.101	0.141
T_c	38.2(1)	37.0(5)	31.4(5)	27.6(1)
H_{c2}^{c}	29.5(1)	30.5(2)	26(1)	23(1)
H_{c2}^{ab}		130(5)	80(5)	48(1)
ν_c	1.26(1)	1.36(1)	1.36(2)	1.2(1)
n_c	2(0)	2.0(0)	2(0)	2(0)
ν_{ab}		1.50(5)	1.45(1)	1.54(7)
n_{ab}		2(0)	2(0)	2(0)

tal data only inside the intervals [26 K, T_c], [18 K, T_c], and [8 K, T_c] for $x=0.013$, 0.101, and 0.141, respectively. For lower temperatures, the estimation of γ is based on the theoretical values of $H_{c2}^{ab}(T)$. Interestingly, γ reduces with x but maintains the temperature dependence. Similarly with pristine MgB_2, γ for $x=0.013$, 0.101, and 0.141 samples is a decreasing function of temperature. Comparing our results to those of Kim and co-workers[33] we find that our crystals with $x=0.101$ and 0.141 have approximately the same T_c with the crystals $x=0.12$ and 0.21, respectively, of Ref. 33. In agreement with those results our high aluminum content crystals show a decreasing of $H_{c2}^{c}(0)$. Finally, our single-crystal results can help in understanding our early NMR line-shape measurements,[22,23] where while for low Al content we observed an increasing of H_{c2}^{c}, for a few percent higher concentrations H_{c2}^{c} was reduced below 23 kOe.

IV. DISCUSSION

Generally, in a two-band anisotropic superconductor several parameters influence the temperature dependence of the superconducting properties, making a difficult task the isolation of those being relevant with the $Mg_{1-x}Al_xB_2$ compound. In the clean limit[47–50] the Fermi-surface topology, the Fermi-velocities, the matrix of the electron-phonon constants λ_{mn}, the Coulomb pseudopotentials μ_{mn} $[m,n=(\sigma,\pi)]$, and the partial density of states $\mathcal{N}_\sigma$ and $\mathcal{N}_\pi$ determine the upper critical fields $H_{c2}^{ab,c}$, the anisotropy parameters $(\gamma_\xi,\gamma_\lambda)$, and T_c. On the other hand, in the dirty limit regime, it has been demonstrated[51,52] that the temperature variation of $H_{c2}^{ab,c}$ and anisotropy parameters are controlled both from interband and intraband scattering rates, provided that λ_{mn}, $\mathcal{N}_\sigma$, and $\mathcal{N}_\pi$ do not change upon alloying.

The role of the intraband impurity scattering on the temperature variation of the anisotropy parameter γ has also been emphasized recently by Mansor and Carbotte.[48] According to their theoretical calculations, for the clean π and σ bands the anisotropy parameter is a decreasing function of temperature, changing from 5 at $T=0$ to less than 3 at T_c. At intermediate values of the intraband scattering rate, a nearly temperature-independent curve has been obtained and in the dirty π band case the anisotropy has been theoretically predicted to increase with temperature.

The experimental results of the aluminum substituted MgB_2 could be explained by a simple clean band model.[26,53] The validity of this limit in the $Mg_{1-x}Al_xB_2$ crystals is supported by theoretical calculations[54] and de Haas–van Alphen measurements on crystals from the same source.[55] In this scenario the aluminum substitution "lives" the $Mg_{1-x}Al_xB_2$ in the clean limit although the mean free path reduces by a factor of 2–3, depending on the examined band.[55] Basically, aluminum substitution results in two changes in the electronic structure of the MgB_2. The first is band filling (shifting of the Fermi level which decreases the hole density of states and shrinks the cylindrical Fermi surface) and the second is increasing the carrier scattering rate (which is related to the increase of residual resistivity). In the case of $Mg_{1-x}Al_xB_2$ (Ref. 31) the resistivity at T_c increases from $\rho_{ab}\sim 0.5$ $\mu\Omega$ cm for $x=0$ crystal, by a factor of 5 for the crystal $x=0.141$. Therefore this reduction is expected to lead to an equal size reduction of the mean free path ℓ. Since $\ell=600$ Å for $x=0$, for crystals of the same source, ℓ is expected to be 200 Å for $x=0.141$. Consequently, most probably $Mg_{1-x}Al_xB_2$ crystals belong to the border of the dirty-clean limit especially as far the π band is concerned.

For low aluminum content we observed a significant reduction of the H_{c2}^{ab} and an almost constant behavior of H_{c2}^{c}. In the clean limit the critical fields of MgB_2 at low temperature are determined mainly by the σ bands.[26,53] In this limit the upper critical field and the coherence length anisotropy are given from the relations $H_{c2}^{c}(0)\propto[\Delta_\sigma(0)/v_\sigma^{ab}]^2$, $H_{c2}^{ab}(0)\propto[\Delta_\sigma^2(0)/v_\sigma^{ab}v_\sigma^{c}]$, and $\gamma_\xi=v_\sigma^{ab}/v_\sigma^{c}$. Here $v_\sigma^{ab,c}$ is defined as the root-mean-squared wave-vector-dependent Fermi velocity in the ab plane (c axis) averaged over the σ sheets of the Fermi surface, and $\Delta_\sigma(0)$ is the σ superconducting gap. In order to interpret the reduction of the anisotropy parameter, we can consider that v_σ^{ab} reduces with aluminum, while v_σ^{c} remains approximately constant. On the other hand, the constancy of the $H_{c2}^{c}(0)$ requires that both Δ_σ and v_σ^{ab} decrease with aluminum. The reduction of Δ_σ with aluminum is reasonable as connected with T_c reduction. This simple model does not agree with the slight increasing of H_{c2}^{c}, in comparison with the pristine MgB_2 for the crystal with the lower aluminum concentration ($x=0.013$). This behavior could be explained in the context of this simple model supposing that both Δ_σ and v_σ^{ab} have lower values, in comparison to the pristine MgB_2, but their ratio gives a value leading to a slightly higher $H_{c2}^{c}(0)$.

The next issue we would like to discuss is the influence of the aluminum substitution on the vortex matter properties. The first attempt in explaining the peak effect in the critical current was made by Pippard, attributing the abrupt increasing of the critical current to the better accommodation of the vortex lattice at the pinning centers, due to the softening of the shear modulus on approaching the second critical field. More than two decays later Larkin and Ovchinnikov[56] refined the original Pippard's suggestion by proposing that the peak effect arises from the sudden softening of the vortex lattice elastic moduli occurring at the crossover from local to nonlocal elasticity near $H_{c2}(T)$.[57] This idea was further enriched by Giamarchi and Le Doussal by proposing that the onset of the peak effect is associated with the proliferation of

dislocations in the flux line lattice, marking a transition from a phase of almost ordered flux lines (termed as Bragg glass) to an amorphous one.[58]

The "disparity" between σ and π bands suppresses the impurity interband scattering that causes pair breaking. Therefore in order for a small region of the crystal with higher x, in respect to the average value, to act as a pinning center, special requirements are needed (see Refs. 7 and 54, and references therein). As we see below, aluminum induced defects do not act as strong pinning centers. For a defect to act as a pinning center it is necessary for its size to be of the order of ξ_{GL}. The crystals used in this work have $\xi_{GL}=26$, 39, and 59 Å, for $x=0.013$, 0.101, and 0.141, respectively. At present it is puzzling why extended Al rich defects (see below) do not act as pinning centers. The fundamental difference between a multiband superconductor and a conventional *s*-wave one-band superconductor, as far as the substitution effects are concerned, is that nonmagnetic impurities may act as Cooper pair breakers due to the interband scattering which mixes the Cooper pairs in the two different bands.[5] Nevertheless, this effect is extremely small in the case of MgB_2 (due to the "disparity" of the σ and π bands preserved even in heavily substituted MgB_2 samples). The onset of the peak effect line practically remains unshifted and the critical current at the peak field slightly reduces with aluminum content. If the aluminum atoms cause significant increasing of the interband scattering between σ and π bands, because of the simultaneous increasing of the size and the number of the pinning centers, then it is reasonable that an important downwards shifting of the onset peak-effect line (H_{on} from the H_{c2}^c) will be expected. This shifting was not clearly observed, implying that the aluminum atoms do not induce appreciable interband scattering, which in turn would produce pinning centers. Consequently, the overall appearance of the peak effect in aluminum substituted crystals leads us to conclude that the extended defects produced by aluminum substitution do not act as pinning centers. The peak effect is most probably related to some other kind of defects, such as vacancies, stacking faults, and dislocations.

Let us discuss here the multiple maximum in the critical current occurring at the regime where the peak effect is observed. Two peaks in the critical current have also been observed in Hg-1201, Y-123, and Tl-2212 superconductors.[42,59–62] If randomly distributed pinning centers exist then the complex appearance of the peak effect is unexpected. The observed behavior could be explained by assuming the existence of pinning centers with different pinning strengths, homogeneously distributed or spatially separated in the bulk of the crystal. This interpretation has been used in the case of the untwinned Y-123 compound[60] where some remaining twin planes are always present, creating planar disorder, in addition to the pointlike oxygen vacancies. Nevertheless, the situation where the crystal contains two types of defects, uniformly distributed in the entire crystal volume, cannot be excluded, e.g., clustering of Al atoms, Mg, and/or Al vacancies, dislocation networks, and extended defects. It has been reported[31] that in crystals having been grown with the same method as the ones studied in this work, a second phase of composition $MgAlB_4$ segregates as a precipitation along the c axis of the crystal. In addition, high-resolution transmission electron *Z*-contrast images revealed precipitations of a second phase in the *form of Al-rich domains* with a broad distribution of sizes and shapes.[31] Most probably, all these experimental facts infer that the double peak effect arises from these inhomogeneities.

V. CONCLUSIONS

We have constructed experimentally the vortex matter phase diagram for three aluminum doped $Mg_{1-x}Al_xB_2$ ($x=0.013$, 0.101, and 0.141) single crystals. All crystals display the peak effect, which for the lower Al content splits into two main distinct peaks. The $H_{c2}^c(0)$ increases slightly only for the $x=0.013$ crystal, while it decreases for the crystals with $x=0.101$ and $x=0.141$, in comparison to the pristine MgB_2. The influence of the Al content on the electronic structure of MgB_2 was also discussed regarding (i) the band filling and (ii) the increasing of the carrier scattering rate. Finally, concerning the peak effect we report several similarities with the high-T_c and low-T_c superconductors, implying that this effect may be effectually explained by employing the same mechanism in all cases.

[1] J. Nagamatsu, N. Nakagawa, T. Muranaka, Y. Zenitani, and J. Akimitsu, Nature (London) **410**, 63 (2001).

[2] J. Kortus, I. I. Mazin, K. D. Belashchenko, V. P. Antropov, and L. L. Boyer, Phys. Rev. Lett. **86**, 4656 (2001).

[3] Y. Wang, T. Plackowski, and A. Junod, Physica C **355C**, 179 (2001).

[4] M. Angst, R. Puzniak, A. Wisniewski, J. Jun, S. M. Kazakov, J. Karpinski, J. Roos, and H. Keller, Phys. Rev. Lett. **88**, 167004 (2002).

[5] A. A. Golubov and I. I. Mazin, Phys. Rev. B **55**, 15146 (1997).

[6] S. C. Erwin and I. I. Mazin, Phys. Rev. B **68**, 132505 (2003).

[7] I. I. Mazin, O. K. Andersen, O. Jepsen, O. V. Dolgov, J. Kortus, A. A. Golubov, A. B. Kuzmenko, and D. van der Marel, Phys. Rev. Lett. **89**, 107002 (2002).

[8] K. Papagelis, J. Arvanitidis, S. Margadonna, Y. Iwasa, T. Takenobu, M. Pissas, and K. Prassides, J. Phys.: Condens. Matter **14**, 7363 (2002).

[9] M. Avdeev, J. D. Jogensen, R. A. Ribero, S. L. Bud'ko, and P. C. Canfield, Physica C **387**, 301 (2003).

[10] P. Samuely, Z. Holanova, P. Szabo, J. Kacmarcik, R. A. Ribeiro, S. L. Bud'ko, and P. C. Canfield, Phys. Rev. B **68**, 020505(R) (2003).

[11] R. H. T. Wilke, S. L. Bud'ko, P. C. Canfield, D. K. Finnemore, R. J. Suplinskas, and S. T. Hannahs, Phys. Rev. Lett. **92**, 217003 (2004).

[12] H. Schmidt, K. E. Gray, D. G. Hinks, J. F. Zasadzinski, M. Avdeev, J. D. Jorgensen, and J. C. Burley, Phys. Rev. B **68**, 060508(R) (2003).

[13] R. Ribeiro, S. L. Bud'ko, C. Petrovic, and P. C. Canfield, Physica C **384**, 227 (2003).

[14] R. H. T. Wilke, S. L. Bud'ko, P. C. Canfield, D. K. Finnemore, and S. T. Hannahs, Physica C **432**, 193 (2005).
[15] M. Pissas, D. Stamopoulos, S. Lee, and S. Tajima, Phys. Rev. B **70**, 134503 (2004).
[16] E. Ohmichi, T. Masui, S. Lee, S. Tajima, and T. Osada, J. Phys. Soc. Jpn. **73**, 2065 (2004).
[17] E. Ohmichi, E. Komatsu, T. Masui, S. Lee, S. Tajima, and T. Osada, Phys. Rev. B **70**, 174513 (2004).
[18] S. M. Kazakov, R. Puzniak, K. Rogacki, A. V. Mironov, N. D. Zhigadlo, J. Jun, C. Soltmann, B. Batlogg, and J. Karpinski, Phys. Rev. B **71**, 024533 (2005).
[19] R. Puzniak, M. Angst, A. Szewczyk, J. Jun, S. M. Kazakov, and J. Karpinski, arXiv:cond-mat/0404579 (unpublished).
[20] P. Postorino, A. Congeduti, P. Dore, A. Nucara, A. Bianconi, D. DiCastro, S. DeNegri, and A. Saccone, Phys. Rev. B **65**, 020507(R) (2001); B. Renker, K. B. Bohnen, R. Heid, D. Ernst, H. Schober, M. Koza, P. Adelmann, P. Schweiss, and T. Wolf, Phys. Rev. Lett. **88**, 067001 (2002).
[21] P. Postorino, A. Congeduti, P. Dore, A. Nucara, A. Bianconi, D. Di Castro, S. De Negri, and A. Saccone, Phys. Rev. B **65**, 020507(R) (2001).
[22] G. Papavassiliou, M. Pissas, M. Karayanni, M. Fardis, S. Koutandos, and K. Prassides, Phys. Rev. B **66**, 140514(R) (2002).
[23] M. Pissas, G. Papavassiliou, M. Karayanni, M. Fardis, I. Maurin, I. Margiolaki, K. Prassides, and C. Christides, Phys. Rev. B **65**, 184514 (2002);
[24] V. Likodimos, S. Koutandos, M. Pissas, G. Papavassiliou, and K. Prassides, Europhys. Lett. **61**, 116 (2003).
[25] M. Putti, M. Affronte, P. Manfrinetti, and A. Palenzona, Phys. Rev. B **68**, 094514 (2003).
[26] M. Putti, C. Ferdeghini, M. Monni, I. Pallecchi, C. Tarantini, P. Manfrinetti, A. Palenzona, D. Daghero, R. S. Gonnelli, and V. A. Stepanov, Phys. Rev. B **71**, 144505 (2005).
[27] M. Ortolani, D. Di Castro, P. Postorino, I. Pallecchi, M. Monni, M. Putti, and P. Dore, Phys. Rev. B **71**, 172508 (2005).
[28] S. V. Barabash and D. Stroud, Phys. Rev. B **66**, 012509 (2002).
[29] O. de la Pena, A. Aguayo, and R. de Coss, Phys. Rev. B **66**, 012511 (2002).
[30] S. Margadonna, K. Prassides, I. Arvanitidis, M. Pissas, G. Papavassiliou, and A. N. Fitch, Phys. Rev. B **66**, 014518 (2002).
[31] J. Karpinski, N. D. Zhigadlo, G. Schuck, S. M. Kazakov, B. Batlogg, K. Rogacki, R. Puzniak, J. Jun, E. Müller, P. Wägli, R. Gonnelli, D. Daghero, G. A. Ummarino, and V. A. Stepanov, Phys. Rev. B **71**, 174506 (2005).
[32] M. Pissas, S. Lee, A. Yamamoto, and S. Tajima, Phys. Rev. Lett. **89**, 097002 (2002); L. Lyard, P. Samuely, P. Szabo, T. Klein, C. Marcenat, L. Paulius, K. H. P. Kim, C. U. Jung, H.-S. Lee, B. Kang, S. Choi, S.-I. Lee, J. Marcus, S. Blanchard, A. G. M. Jansen, U. Welp, G. Karapetrov, and W. K. Kwok, Phys. Rev. B **66**, 180502(R) (2002); U. Welp, A. Rydh, G. Karapetrov, W. K. Kwok, G. W. Crabtree, Ch. Marcenat, L. Paulius, T. Klein, J. Marcus, K. H. P. Kim, C. U. Jung, H.-S. Lee, B. Kang, and S.-I. Lee, Phys. Rev. B **67**, 012505 (2003); M. Angst, R. Puzniak, A. Wisniewski, J. Jun, S. M. Kazakov, and J. Karpinski, Phys. Rev. B **67**, 012502 (2003).
[33] Heon-Jung Kim, Hyan-Sook Lee, Byeongwon Kang, Woon-Ha Yim, Younghun Jo, Myung-Hwa Jung, and Sung-Ik Lee, Phys. Rev. B **73**, 064520 (2006).
[34] M. Angst, R. Puzniak, A. Wisniewski, J. Jun, S. M. Kazakov, and J. Karpinski, Phys. Rev. B **67**, 012502 (2003).
[35] X. S. Ling, S. R. Park, B. A. McClain, S. M. Choi, D. C. Dender, and J. W. Lynn, Phys. Rev. Lett. **86**, 712 (2001).
[36] A. A. Gapud, D. K. Christen, J. R. Thompson, and M. Yethiraj, Phys. Rev. B **67**, 104516 (2003).
[37] Maria G. Adesso, Davide Uglietti, René Flükiger, Massimiliano Polichetti, and Sandro Pace, Phys. Rev. B **73**, 092513 (2006).
[38] S. Bhattacharya and M. J. Higgins, Phys. Rev. B **49**, 10005 (1994), and references therein.
[39] M. Marchevsky, M. J. Higgins, and S. Bhattacharya, Nature (London) **409**, 591 (2001).
[40] T. Klein, I. Joumard, S. Blanchard, J. Marcus, R. Cubitt, T. Giamarchi, and P. Le Doussal, Nature (London) **413**, 404 (2001).
[41] N. Avraham, B. Khaykovich, Y. Myasoedov, M. Rappaport, H. Shtrikman, D. E. Feldman, T. Tamegai, P. H. Kes, M. Li., M. Konczykowski, K. van der Beek, and E. Zeldov, Nature (London) **411**, 451 (2001).
[42] D. Stamopoulos and M. Pissas, Phys. Rev. B **65**, 134524 (2002); Supercond. Sci. Technol. **14**, 844 (2001).
[43] W. K. Kwok, J. A. Fendrich, C. J. van der Beek, and G. W. Crabtree, Phys. Rev. Lett. **73**, 2614 (1994), and references therein.
[44] D. Stamopoulos, M. Pissas, and A. Bondarenko, Phys. Rev. B **66**, 214521 (2002).
[45] A. A. Zhukov, S. Kokkaliaris, P. A. J. de Groot, M. J. Higgins, S. Bhattacharya, R. Gagnon, and L. Taillefer, Phys. Rev. B **61**, R886 (2000).
[46] S. O. Valenzuela and V. Bekeris, Phys. Rev. Lett. **84**, 4200 (2000); **86**, 504 (2001).
[47] M. E. Zhitomirsky and V.-H. Dao, Phys. Rev. B **69**, 054508 (2004).
[48] M. Mansor and J. P. Carbotte, Phys. Rev. B **72**, 024538 (2005).
[49] T. Dahm and N. Schopohl, Phys. Rev. Lett. **91**, 017001 (2003).
[50] P. Miranović, K. Machida, and V. G. Kogan, J. Phys. Soc. Jpn. **72**, 221 (2003).
[51] A. Gurevich, Phys. Rev. B **67**, 184515 (2003).
[52] A. A. Golubov and A. E. Koshelev, Phys. Rev. B **68**, 104503 (2003).
[53] M. Angst, S. L. Bud'ko, R. H. T. Wilke, and P. C. Canfield, Phys. Rev. B **71**, 144512 (2005).
[54] J. Kortus, O. V. Dolgov, R. K. Kremer, and A. A. Golubov, Phys. Rev. Lett. **94**, 027002 (2005).
[55] A. Carrington, J. D. Fletcher, J. R. Cooper, O. J. Taylor, L. Balicas, N. D. Zhigadlo, S. M. Kazakov, J. Karpinski, J. P. H. Charmant, and J. Kortus, Phys. Rev. B **72**, 060507(R) (2005).
[56] A. I. Larkin and Yu. N. Ovchinnikov, J. Low Temp. Phys. **34**, 409 (1979).
[57] E. H. Brandt, J. Low Temp. Phys. **26**, 709 (1977).
[58] T. Giamarchi and P. Le Doussal, Phys. Rev. B **55**, 6577 (1997).
[59] M. Pissas, D. Stamopoulos, V. Psycharis, Y. C. Ma, and N. L. Wang, Phys. Rev. B **73**, 174524 (2006).
[60] D. Pal, S. Ramakrishnan, A. K. Grover, D. Dasgupta, and Bimal K. Sarma, Phys. Rev. B **63**, 132505 (2001); L. Miu, *ibid.* **65**, 096501 (2002); D. Pal, S. Ramakrishnan, and A. K. Grover, *ibid.* **65**, 096502 (2002).
[61] A. I. Rykov, *Studies of High Temperature Superconductors*, edited by Anant Narlikar (Nova Science Publishers Inc., 2000), Vol. 31, p. 149.
[62] T. Nishizaki, K. Shibata, T. Sasaki, and N. Kobayashi, Physica C **341–348**, 957 (2000).